

A model of the TeV flare of Cygnus X-1: electron acceleration and extended pair cascades

Andrzej A. Zdziarski,¹★ Julien Malzac²★ and W. Bednarek³★

¹*Centrum Astronomiczne im. M. Kopernika, Bartycka 18, 00-716 Warszawa, Poland*

²*CESR, OMP, UPS, CNRS; 9 Avenue du Colonel Roche, BP4346, 31028 Toulouse Cedex 4, France*

³*Department of Experimental Physics, University of Łódź, 90-236 Łódź, Poland*

5 March 2019

ABSTRACT

We consider theoretical models of emission of TeV photons by Cyg X-1 during a flare discovered by the MAGIC detector. We study acceleration of electrons to energies sufficient for TeV emission, and find the emission site is allowed to be close to the black hole. We then consider pair absorption in the photon field of the central X-ray source and a surrounding accretion disc, and find its optical depth is $\lesssim 1$, allowing emission close to the black hole. On the other hand, the optical depth in the stellar field is ~ 10 at ~ 1 TeV. However, the optical depth drops with increasing energy, allowing a model with the initial energy of $\gtrsim 3$ TeV, in which photons travel far away from the star, initiating a spatially extended pair cascade. This qualitatively explains the observed TeV spectrum, though still not its exact shape.

Key words: accretion, accretion discs – radiation mechanisms: non-thermal – stars: individual: Cyg X-1 – stars: individual: HDE 226868 – X-rays: binaries – X-rays: stars.

1 INTRODUCTION

The black-hole binary Cyg X-1 is at present the only X-ray binary that is both certainly accretion-powered and from which very high energy γ -rays, $\gtrsim 0.1$ TeV, have been detected by one of the current generation of TeV detectors. Namely, a transient TeV emission was detected by the MAGIC telescope (Albert et al. 2007, hereafter A07). Among the three other currently known TeV-emitting binaries (which are all persistent in the TeVs except for orbital variations), PSR B1259–63 (Aharonian et al. 2005) is known to be powered by the rotation energy of a young pulsar rather than by accretion (Johnston et al. 1992), with the resulting interaction of the pulsar and stellar winds leading to production of energetic photons (Maraschi & Treves 1981). Then, LS I +61°303 (Albert et al. 2006) is very likely of the same nature, as indicated by its radio observations showing a cometary-tail-like variable structure rather than a jet (Dhawan et al. 2006). A further very strong evidence for the presence of a young pulsar in that system is provided by a detection of a powerful ~ 0.2 -s flare with the peak 15–150 keV flux of $\simeq 5 \times 10^{-8}$ erg cm^{−2} s^{−1} (which is higher by a factor of $\sim 10^3$ than the average source flux) and a blackbody-like spectrum by the *SWIFT* BAT (De Pasquale et al. 2008; Barthelmy et al. 2008). Such an event is fully consistent with a soft gamma-ray repeater/anomalous X-ray pulsar short duration burst (Dubus & Giebels 2008). Then, the case of LS 5039 (Aharonian et al. 2006) is least clear, but

the striking similarity of the broad-band spectra of all three systems points to similar mechanisms of their activity (Dubus 2006b). All three persistent systems are also similar in being eccentric high-mass binaries containing massive B or O stars. Furthermore, their broad-band spectra are very much unlike those of accreting sources at similar Eddington ratios as well as are unlikely to be dominated by a collimated jet emission (see, e.g., a discussion in Zdziarski et al. 2008).

Then, there were some early claims of TeV emission from accreting X-ray binaries, most notably from Cyg X-3. Its TeV flux was claimed to be very strong and modulated at the orbital period (e.g., Lamb et al. 1982), which, however, was not confirmed by a subsequent Whipple Observatory pointing (Weekes 1983). Cyg X-3 has not, until now, been detected by either the MAGIC, VERITAS, or HESS telescopes.

Thus, the case of TeV emission from Cyg X-1 is of crucial importance for our understanding of emission of γ -rays from accretion flows. The statistical significance of the detected transient was 4.9σ or 4.1σ post-trial (A07), unlikely to appear by chance. Supporting the reality of this transient emission is also the coincidence with a flare of Cyg X-1 seen in X-rays (A07; Türler et al. 2006; Malzac et al. 2008, hereafter M08).

The TeV detection occurred on 2006 September 24, MJD 54002.[928–982] (A07), which corresponds to the orbital phases of 0.90–0.91, i.e., with the black hole behind the companion. No signal was detected (A07) during the first half of that MAGIC observation, MJD 54002.[875–928], indicating time variability of the TeV emission on the time scale of less than an hour. The emission

* E-mail: aaz@camk.edu.pl (AAZ), malzac@cesr.fr (JM), bednar@fizwe4.phys.uni.lodz.pl (WB)

was detected in the 0.15–1 TeV range, and was fitted by a power law with a photon spectral index of $\Gamma = 3.2 \pm 0.6$ (A07). The 0.1–1 TeV isotropic luminosity corresponding to the best fit is $\approx 2 \times 10^{34}$ erg s $^{-1}$ (assuming the distance of $D = 2$ kpc, see Ziółkowski 2005 and references therein). The MAGIC telescope also observed, but did not detect, Cyg X-1 on 25 other nights, and obtained an upper limit to the flux vs. energy an order of magnitude below the flux during the flare (A07).

As mentioned above, the TeV flare occurred during a longer X-ray outburst. Based on data from the *RXTE* All Sky Monitor (ASM), the X-ray flare lasted three days, about MJD 54002.0–54005.0. Cyg X-1 was then in the hard spectral state (M08). The *INTEGRAL* IBIS and SPI instruments observed Cyg X-1 in the 18–700 keV range on MJD 54002.4–54004.3 (M08), during which the estimated bolometric luminosity was $\approx 4 \times 10^{37}$ erg s $^{-1}$. M08 obtained, in particular, the X-ray spectrum for an interval coinciding with the TeV detection. The spatial location of the TeV emission region remains unknown. However, the simplest hypothesis to consider that it was close to the X-ray source. Then, we can calculate e $^{\pm}$ pair absorption of the TeV photons as well as the Compton energy loss of accelerated electrons due to interactions with the X-rays.

2 THE BINARY PARAMETERS AND THE 1 eV–1 MeV SPECTRUM

The system parameters of interest to our study are the stellar temperature, T_* , the stellar radius, R_* , the separation, a , and the inclination, i . The radius of the companion, HDE 226868, and the component masses are subject to a considerable uncertainty, compare, e.g., Herrero et al. (1995) with Ziółkowski (2005). Here, we adopt the best model of Herrero et al. (1995), with $R_* = 1.2 \times 10^{12}$ cm, the separation of $a = 2.47R_*$, and $T_* \approx 3.2 \times 10^4$ K. The observed stellar flux is plotted in Fig. 1. The value of the inclination of Cyg X-1 is relatively uncertain; here, we adopt $i = 30^\circ$ (e.g., Gies & Bolton 1986).

The 18–700 keV X-ray spectrum during the TeV flare was fitted by M08 as an e-folded power law. Physically, it corresponds to thermal Comptonization of blackbody photons produced at the inner edge of a cold disc, which temperature is measured as $kT_{\text{bb,max}} \approx 0.3$ keV (Frontera et al. 2001). At low energies, the spectrum has a low-energy break, with the Rayleigh-Jeans form below the break. To model it, we assume the observed broad-band energy flux, F_h , is given by,

$$EF_h(E) = \frac{K(E_b/1 \text{ keV})^{2-\Gamma} \exp(-E/E_c)}{(E/E_b)^{-3} + (E/E_b)^{\Gamma-2}}, \quad (1)$$

which has the form of $KE^{2-\Gamma} \exp(-E/E_c)$ at $E \gg E_b$. We assume $E_b = 0.3$ keV ($\sim kT_{\text{bb}}$). For the remaining parameters, we use the best-fit parameters of M08, $\Gamma = 1.34$, $E_c = 111$ keV, $K = 1.25$ keV cm $^{-2}$ s $^{-1}$. This spectrum is plotted in Fig. 1.

The corresponding photon density within the central hot source, $n_h(E)$, can be calculated by assuming an isotropic and homogeneous spherical source with the radius, R_h , in which the average photon escape time is $3R_h/4c$,

$$E^2 n_h(E, R_h) \approx \frac{9D^2 EF_h(E)}{4R_h^2 c}. \quad (2)$$

The hard state emission is well modelled as coming from a hot inner flow surrounded by a cold disc truncated at ~ 30 – $100R_g$, where R_g is the gravitational radius (e.g., Done et al. 2007). For the black hole

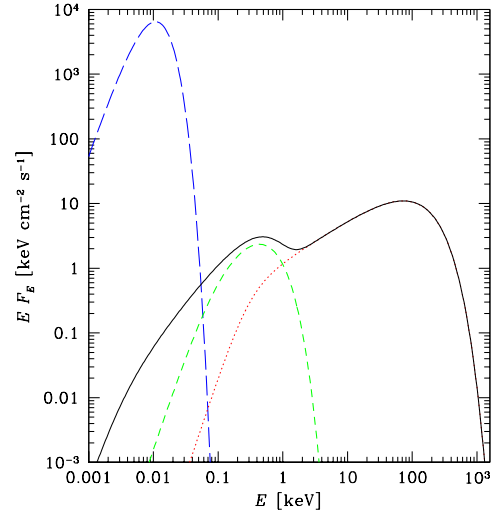


Figure 1. The spectral components of the Cyg X-1/HDE 226868 system. The logn dashes give the blackbody spectrum of the OB supergiant (for the parameters of Herrero et al. 1995). The dotted curve gives the thermal Comptonization component from the hot inner flow. The short dashes give the spectrum of the inner disc of the surrounding optically-thick disc, and the solid curve gives the spectrum of the entire disc (tidally truncated at the outer radius) together with the hot-plasma emission. See Section 2 for details.

mass of $M_X \sim 10M_\odot$, the radius of the inner hot flow is $R_h \sim 10^8$ cm, which value we assume hereafter.

Moving away from the hot plasma, the local photon density includes an increasing number of soft photons from the surrounding disc. For a given height above the disc, most of the photons come from the part of the disc within the radius equal to the height. For our calculations below, we consider logarithmically spaced parts of the outer disc. The inner disc temperature is $kT_{\text{bb,max}} \approx E_b \approx 0.3$ keV, with which factor the spectrum is exponentially cut off at high energies. The temperature decreases with the increasing radius as $T_{\text{bb}} \propto R^{-1/2}$, and the resulting disc blackbody spectrum is $F_d(E) \propto E^{1/3}$. At the outer edge of the considered region, R_{out} , the local spectrum changes to the Rayleigh-Jeans one. The corresponding energy is $E_{\text{out}} = (R_{\text{out}}/R_h)^{-1/2} E_b$. Thus, we approximate the disc spectrum by,

$$EF_d(E, R_{\text{out}}) = \frac{K' E_{\text{out}}^{4/3} \exp(-E/E_b)}{(E/E_{\text{out}})^{-3} + (E/E_{\text{out}})^{-4/3}}, \quad (3)$$

where the normalization constant, K' , follows from the condition that F_d and F_h intersect at some energy, which we choose as 1 keV based on the fits to *BeppoSAX* data in Frontera et al. (2001). This choice also reproduces the soft excess appearing in the hard state of Cyg X-1 at $E \lesssim 3$ keV (Gierliński et al. 1997). We then consider the regions with $R_{\text{out}} = 10^9$ cm, 10^{10} cm, 10^{11} cm, and 10^{12} cm. The last value roughly corresponds to the tidal truncation radius in Cyg X-1 (see, e.g., an estimate in Lachowicz et al. 2006). The spectrum of equation (3) for $R_{\text{out}} = 10^9$ cm and the total spectrum of the disc and the hot flow are plotted in Fig. 1. The disc photon density, $n_d(E, R_{\text{out}})$, is approximated analogously to equation (2),

$$E^2 n_d(E, R_{\text{out}}) \approx 9D^2 EF_d(E, R_{\text{out}})/(4R_{\text{out}}^2 c). \quad (4)$$

We have tested the form of the total spectrum against the *RXTE*/ASM measurements, as given in M08, who used a conversion matrix of Zdziarski et al. (2002) for the average (during the *INTEGRAL* observation) ASM count rates in the three channels of

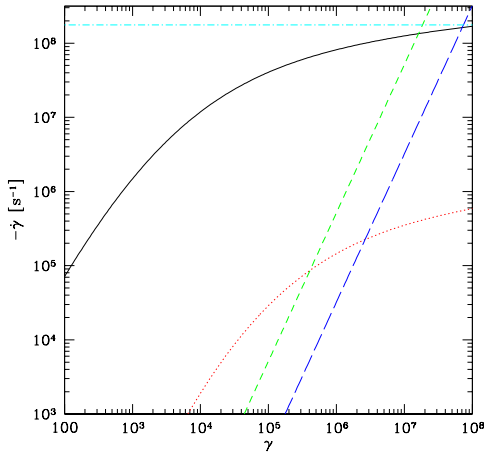


Figure 2. The Compton energy loss rate, $-\dot{\gamma}$, in the X-ray photon field, given by equations (1–4) and assuming the radius of 10^9 cm (solid curve), and in the stellar field diluted at the position of the black hole (dotted curve). The synchrotron loss rate is shown for $B = 20$ G (short dashes), and for $B = 5$ G (long dashes), and the dot-dashed line is (–) the acceleration rate, equation (5) for $B = 20$ G and $\xi = 0.5$.

the detector to energy fluxes. As found by M08, the average flux level was close to that during the TeV flare. We have found that the resulting energy fluxes in the 1.5–3 keV, 3–5 keV and 5–12 keV ranges agree with those obtained by integration of our total spectrum to within ~ 30 per cent. This confirms the overall correctness of our spectral form.

3 ELECTRON ACCELERATION

Here, we consider whether electrons can be accelerated to TeV energies within or close to the central X-ray source. We consider the acceleration rate in a generic form, applicable, e.g., to shock acceleration,

$$\dot{\gamma}_{\text{acc}} = \frac{\xi c \gamma}{r_L} = \frac{\xi e B}{m_e c} \approx 1.8 \times 10^7 \xi \frac{B}{1 \text{ G}} \text{ s}^{-1}, \quad (5)$$

where γ is the Lorentz factor, $r_L = \gamma m_e c^2 / e B \approx 1700 \gamma / B$ cm is the Larmor radius, B is the magnetic field strength, e is the electron charge, and $\xi \lesssim 1$ is a dimensionless quantity parameterizing the acceleration efficiency (see, e.g., Bednarek & Giovannelli 2007¹). The maximum electron Lorentz factor can be then obtained for the acceleration rate being equal to an energy loss rate.

The synchrotron energy loss is given by,

$$-\dot{\gamma}_S = \frac{4}{3} \frac{\sigma_T}{m_e c} \frac{B^2}{8\pi} \gamma^2 \approx 1.3 \times 10^{-9} \gamma^2 \left(\frac{B}{1 \text{ G}} \right)^2 \text{ s}^{-1}. \quad (6)$$

Equating this loss rate to the acceleration rate, equation (5), we obtain the corresponding maximum Lorentz factor of

$$\gamma_{\text{max,S}} = \left(\frac{6\pi \xi e}{\sigma_T B} \right)^{1/2} \approx 1.2 \times 10^8 \xi^{1/2} \left(\frac{B}{1 \text{ G}} \right)^{-1/2}. \quad (7)$$

¹ Note that there is a spurious factor of π in eq. (3) of Bednarek & Giovannelli (2007), which results in an underestimate of the Lorentz factor in their eq. (7), and the -2 factor in their eq. (6) should be outside the argument of the logarithm. Also, we note that in Bednarek (1997), μ denotes $-\cos$ between the directions of the interacting photons.

In addition, if electrons are accelerated within the hot plasma region, the Larmor radius has to be smaller than the acceleration site size, R_{acc} , which yields the maximum Lorentz factor of

$$\gamma_{\text{max,L}} = \frac{B R_{\text{acc}} e}{m_e c^2} \approx 6 \times 10^5 \frac{B}{1 \text{ G}} \frac{R_{\text{acc}}}{10^9 \text{ cm}}. \quad (8)$$

Then, comparing equations (7) and (8), we obtain the optimum magnetic field yielding the highest maximum the Lorentz factor subject to both constraints together,

$$B_{\text{opt}} = \left(\frac{6\pi \xi m_e^2 c^4}{R_{\text{acc}}^2 e \sigma_T} \right)^{1/3} \approx 35 \xi^{1/3} \left(\frac{R_{\text{acc}}}{10^9 \text{ cm}} \right)^{-2/3} \text{ G}, \quad (9)$$

which Lorentz factor equals

$$\gamma_{\text{max}} = \left(\frac{6\pi e^2 \xi R_{\text{acc}}}{m_e c^2 \sigma_T} \right)^{1/3} \approx 2 \times 10^7 \xi^{1/3} \left(\frac{R_{\text{acc}}}{10^9 \text{ cm}} \right)^{1/3}. \quad (10)$$

We see that the optimum magnetic field is relatively weak, e.g., $\approx 160 \xi^{1/3}$ G if $R_{\text{acc}} = R_h = 10^8$ cm. The magnetic field expected in the hot inner plasma from equipartition arguments is considerably higher, $B \gtrsim 10^5$ G (e.g., Malzac & Belmont 2008). Thus, the preferred acceleration site is outside of the hot inner plasma. It can be, e.g., a shock region where the stellar wind collides with the hot inner flow, or an inner part of the jet. The Lorentz factor of the accelerated electrons is completely sufficient to account for the photon energies observed in the TeV flare. In fact, the maximum Lorentz factor can still be lower than that of equation (10), which will then allow a value of the magnetic field higher than that of equation (9).

An important process is also the loss rate due to Compton scattering with the X-ray and disc photons, equations (1–4), and due to the stellar photon density at the position of the black hole. For simplicity, we assume isotropic photon fields. The energy loss of electrons with $\gamma^2 \gg 1$ in scattering with isotropic photons of an arbitrary energy is given by Jones (1968) (see also eq. A30 in Zdziarski 1988). We integrate this rate over the photon density assuming the source size of 10^9 cm, obtaining the $-\dot{\gamma}$ shown in Fig. 2. We see that if the magnetic field is given by equation (9), the Compton energy loss rate around γ_{max} (which is in the Klein-Nishina limit) is comparable to that due to the synchrotron losses. Thus, they would only slightly affect our estimates above. Also, we see that the losses on the X-rays dominate over those on the stellar photons.

Thus, we find the conditions around the X-ray source to allow electron acceleration up to the Lorentz factor of $\sim 10^7$, which then easily allows emission of photons in the TeV range. The acceleration time scale, $\gamma/\dot{\gamma}$, is then very short, $\gtrsim 1$ s, see equation (5).

4 PAIR ABSORPTION OF TeV EMISSION

Pair absorption of the TeV photons in photon-photon e^+e^- pair production events is a major issue in interpretation of the TeV flare. In a study of pair absorption by photons from the companion star, Bednarek & Giovannelli (2007) found that TeV photons should be preferentially observed from Cyg X-1 at the orbital phases of 0.45–0.55, i.e., near the inferior conjunction, which is almost exactly opposite to the phase of the observed event. However, pair absorption can also take place on size scales much smaller than the system separation, due to pair-production events with the intense X-ray field of the central source. Below, we consider separately interaction with the X-rays and with the stellar photons.

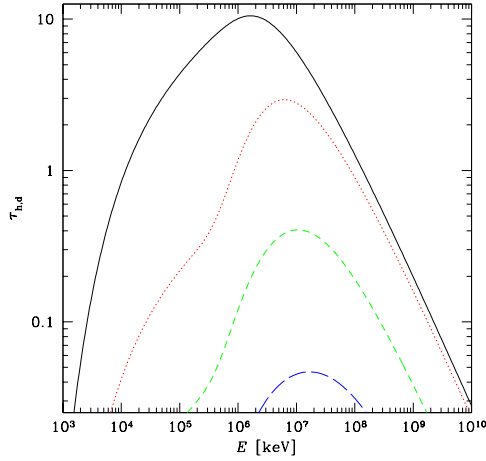


Figure 3. The optical depth to photon-photon pair production in the field of the hot plasma and the disc emission. The four curves from the bottom to top give the contributions of the consecutive decades of the distance above the disc, with the outer boundaries at 10^{11} cm, 10^{10} cm, 10^9 cm, and 10^8 cm (the radius of the inner hot flow). The acceleration site is likely at $\gtrsim 10^9$ cm, Section 3, and thus the TeV photons are unlikely to experience the optical depth of the top curve.

4.1 TeV–X-ray pair absorption

As discussed above, the acceleration site is most likely larger than the hot inner plasma. Still, for completeness we calculate the e^\pm pair absorption optical depth across the inner hot plasma, with the size of R_h ,

$$\tau_h(E_\gamma, R_h) = R_h \int_{m_e^2 c^4 / E_\gamma}^{\infty} n_h(E) \bar{\sigma}_{\gamma\gamma}[(E_\gamma E)^{1/2}] dE \propto R_h^{-1}, \quad (11)$$

where $\bar{\sigma}_{\gamma\gamma}$ is the cross section averaged over isotropic target photons (Gould & Schröder 1967; corrected in Brown et al. 1973b; see also eqs. B11–B13 in Zdziarski 1988). The resulting optical depth is shown in Fig. 3. We see that whereas it is $\gtrsim 1$ in the ~ 0.01 – 100 GeV range, the (Klein–Nishina) high-energy decline of the cross section results in $\tau_h \lesssim 1$ above this range.

We then consider pair absorption above the disc. Studies of this problem were given by Carramiñana (1992) and Bednarek (1993), but they considered discs extending to the minimum stable orbit and were given as numerical simulations, so we cannot use them here. The optical depth within each of the outer disc region considered in Section 2 is calculated using,

$$\tau_d(E_\gamma, R_{\text{out}}) = \frac{R_{\text{out}}}{2} \int_{m_e^2 c^4 / E_\gamma}^{\infty} [n_d(E, R_{\text{out}}) + n_h(E)] \bar{\sigma}_{\gamma\gamma}[(E_\gamma E)^{1/2}] dE, \quad (12)$$

i.e., we take into account contribution from the Comptonization photons to the opacity in each of the regions. Note that we have employed the isotropic approximation to the pair opacity whereas the disc blackbody photons are all directed away from the disc and their flux in a given direction is $\propto \cos \phi$, where ϕ is the angle measured with respect to the disc normal. This blackbody-type beaming would substantially decrease the optical depth, and to approximately account for it, we have introduced a factor of $1/2$ in equation (12). The resulting contributions and the total optical depth are shown in Fig. 3. We see that the optical depth in the MAGIC detection range, > 0.15 TeV, is < 1 .

We note that our calculations of the absorption by the disc photons were done in a very simple way. However, given both the disc and TeV photons travelling up above the disc, we expect that

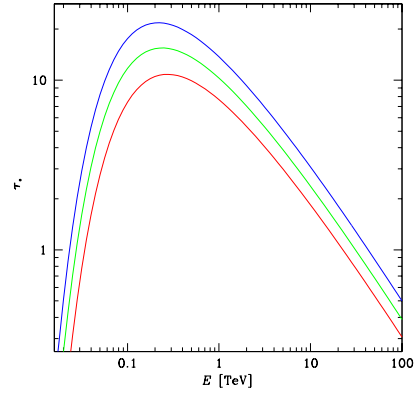


Figure 4. The pair-production optical depth in the field of the star from the location of the black hole up to infinity at the orbital phase of 0.9 and for the inclinations of 30° , 45° and 60° , from bottom to top.

our results give an overestimate of the optical depth rather than an underestimate. We have neglected any pair cascades above the disc, which effect would also be to reduce the effect of the pair opacity. Then, we neglect any irradiation of the outer disc. However, we can see that the outermost part of the disc, where irradiation is likely to be most important, contributes negligibly to the total opacity, and the disc flux would have to be increased by ~ 3 orders of magnitude for its opacity to become important. Summarizing, we have shown that it is entirely possible that photons with energies $\gtrsim 0.1$ TeV escape pair absorption in the vicinity of the X-ray source.

4.2 Pair absorption on stellar photons and spatially extended pair cascades

We accurately calculate the optical depth on stellar photons, taking into account their anisotropy outside the stellar surface. We have used the methods of Bednarek (1997) (with triple integration) and Dubus (2006a) (with quadruple integration) and found they fully agree with each other. The results for the orbital phase of 0.9, the binary parameters given in Section 2, and three values of i are shown in Fig. 4. We see that at $i = 30^\circ$, $\tau_* > 1$ between 40 GeV and 20 TeV. This might have implied that the acceleration process could not have taken place in the black hole vicinity.

However, we note that a similar problem is faced in the case of the TeV-emitting X-ray binary LS 5039. Its parameters, $R_* \approx 6 \times 10^{11}$ cm, $T_* \approx 3.9 \times 10^4$ K, $a \approx 2.2 R_*$, and the eccentricity of $e \approx 0.35$ (Casares et al. 2005), imply a system even more compact and, especially at periastron, more opaque to pair absorption than Cyg X-1. Still, a steady TeV emission is detected from LS 5039 at both the superior conjunction and the periastron (Aharonian et al. 2006), which two points occur very close from each other in the orbital phase in that system. This is contrary to the theoretical predictions based on the pair absorption alone, giving fluxes at those phases much lower than those observed (Dubus 2006a; Bednarek 2006), similarly to the predictions implied by Fig. 4. The solution to this dilemma may be presented by pair cascades. They may be initiated by electrons and photons at energies of ~ 3 – 10 TeV, at which energy the pair optical depth measured from the compact object drops to ~ 1 , implying that those photons can propagate relatively far from the star. The resulting pairs produce photons at lower energies, which then can propagate to the observer in the much diluted blackbody field. Such spatially extended pair cascade model was

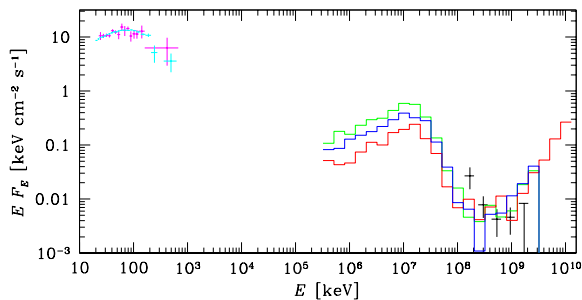


Figure 5. The *INTEGRAL* spectrum from the ISGRI (cyan crosses), PICsIT (the cyan cross at the highest energy) and the SPI (magenta crosses), from M08, simultaneous with the MAGIC spectrum (black crosses, A07). The MAGIC spectrum is compared to the results from our pair cascade models, with the green and histograms corresponding to the primary monoenergetic electron injection at 3.16 TeV and 10 TeV, respectively. The blue histogram is for 3.16 TeV, but with the stellar temperature assumed to be 3.0×10^4 K (which is within the observational uncertainties for Cyg X-1). The normalization of the histograms have been chosen to match the MAGIC data.

applied to LS 5039 by Bednarek (2007). Similar pair cascades can also take place in the X-ray field (see above).

To calculate pair cascades, we use two methods. One is of Bednarek (1997), and the other is an independent Monte Carlo method, which employs the full Klein-Nishina cross section rather than its approximation (used by Bednarek 1997). We have found the two methods give results consistent with each other. We present some of our results in Fig. 5, for monoenergetic electron injection at 3.16 TeV and 10 TeV. This form of injection is supported by results of studies of acceleration including energy losses, see, e.g., Protheroe (2004). We find we can reproduce the MAGIC spectrum only qualitatively. Generally, our models predict too much emission at energies $\gtrsim 1$ TeV, and too little at $\lesssim 0.2$ TeV. We have found this to be a generic problem, and changing the injection energy does not improve the agreement with the data. Some improvement at the low energy end appears when a steep power law injection is added; however, this is at the expense of greatly increasing the intrinsic power of the flare. On the other hand, we consider it possible that, given complications in interpreting Cherenkov telescope data, the actual spectrum of Cyg X-1 was similar to that predicted by our models. The observed 0.1–1 TeV isotropic power is 0.011–0.022 of the the total power injected in TeV electrons, for the three models shown in Fig. 5. This implies an injected power of $\sim 10^{36}$ erg s^{-1} , which is still much less than the bolometric X-ray luminosity, $\simeq 4 \times 10^{37}$ erg s^{-1} (M08).

In our model, we have assumed that the Compton losses of the cascade pairs dominate over the synchrotron losses. This requires that the magnetic field of the star is relatively weak, $B \lesssim 5$ G or so (see Fig. 2) along the line of sight. The magnetic field of HDE 226868 is unknown. In our model, it is required to be weaker than that of strongly-magnetized O stars, where the surface dipole field can reach $\sim 10^3$ G (Wade et al. 2006). This is also pointed out by Bosch-Ramon et al. (2008). We also assume that the pairs of the cascade quickly isotropise after their production, and produce γ -rays via Compton scattering locally, which will be the case even for a very weak field.

An alternative explanation of the observed flare is that the primary TeV emission occurred at a large distance from the black hole, e.g., along its jet, far enough to avoid the pair absorption by the stellar photons (see also Bosch-Ramon et al. 2008). The observed TeV variability (A07) implies the emission region has a size $\lesssim 10a$. The

distance from the black hole needs to be of the order of a few times a (fig. 2 in Bednarek & Giovannelli 2007). Even if it is $\sim 1a$, it corresponds to $\sim 2 \times 10^6 R_g$ for $M = 10 M_\odot$. In the case of blazars, most of the γ -ray emission is considered to come from distances a few orders of magnitude smaller (e.g., Sikora et al. 1994). On the other hand, this has been challenged in some cases, especially for M87, where the TeV emission has been argued to originate at $\gtrsim 120$ pc (Cheung et al. 2007). For the black hole mass of $3 \times 10^6 M_\odot$, this corresponds to $\sim 3 \times 10^5 R_g$, still substantially less than corresponding number for Cyg X-1.

Note that some energy is transported to such distances in Cyg X-1 in its jet, and it appears as radio emission (Stirling et al. 2001). However, the total radio luminosity of Cyg X-1 is only $\sim 10^{31}$ erg s^{-1} (Fender et al. 2000), less than three orders of magnitude than the observed 0.1–1 TeV power, and five orders of magnitude less than the intrinsic cascade power, see above.

5 CONCLUSIONS

We have studied acceleration models for the TeV flare observed from Cyg X-1 by the MAGIC telescope. We have found that spatially extended pair cascades can in principle explain the observations provided the companion star in the system has a weak magnetic field.

ACKNOWLEDGMENTS

We thank G. Dubus, M. Ostrowski and Ł. Stawarz for valuable discussions. This research has been supported in part by the CNRS, the LEA Astrophysics Poland-France (Astro-PF) program, the Polish MNiSW grants NN203065933 and NN203390834, and the Polish Astroparticle Network 621/E-78/SN-0068/2007. We thank the MAGIC collaboration for the Cyg X-1 spectrum in electronic form.

REFERENCES

- Aharonian F. et al., 2005, *A&A*, 442, 1
- Aharonian F. et al., 2006, *A&A*, 460, 743
- Albert J. et al., 2006, *Sci*, 312, 1771
- Albert J. et al., 2007, *ApJ*, 665, L51 (A07)
- Barthelmy S. D., et al., 2008, *GCN*, 8215
- Bednarek W., 1993, *A&A*, 278, 307
- Bednarek W., 1997, *A&A*, 322, 523
- Bednarek W., 2006, *MNRAS*, 368, 579
- Bednarek W., 2007, *A&A*, 464, 259
- Bednarek W., Giovannelli F., 2007, *A&A*, 464, 437
- Bosch-Ramon, V., Khangulyan, D., & Aharonian, F. A., 2008, *A&A*, in press, arXiv:0808.1540
- Brown R. W., Mikaelian K. O., Gould R. J., 1973, *ApL*, 14, 203
- Carramiñana A., 1992, *A&A*, 264, 127
- Casares J., Ribó M., Ribas I., Paredes J. M., Martí J., Herrero A., 2005, *MNRAS*, 364, 899
- Cheung C. C., Harris D. E., Stawarz Ł., 2007, *ApJ*, 663, L65
- De Pasquale M., et al., 2008, *GCN*, 8209
- Dhawan V., Mioduszewski A. J., Rupen M., 2006, in *Proc. of VI Microquasar Workshop, Proceedings of Science*, 52.1
- Done C., Gierliński M., Kubota A., 2007, *A&ARv*, 15, 1
- Dubus G., 2006a, *A&A*, 451, 9
- Dubus G., 2006b, *A&A*, 456, 801

- Dubus G., Giebels, B., 2008, ATel, 1715
- Fender R. P., Pooley G. G., Durouchoux P., Tilanus R. P. J., Brock-sopp C., 2000, MNRAS, 312, 853
- Frontera F., et al., 2001, ApJ, 546, 1027
- Gierliński M., Zdziarski A. A., Done C., Johnson W. N., Ebisawa K., Ueda Y., Haardt F., Philips B. F., 1997, MNRAS, 288, 958
- Gies D. R., Bolton C. T., 1986, ApJ, 304, 371
- Gould R. J., Schröder G. P., 1967, PhRv, 155, 1404
- Herrero A., Kudritzki R. P., Gabler R., Vilchez J. M., Gabler A., 1995, A&A, 297, 556
- Johnston S., Manchester R. N., Lyne A. G., Bailes M., Kaspi V. M., Qiao G., D’Amico N., 1992, ApJ, 387, L37
- Jones F. C., 1968, Phys. Rev., 167, 1159
- Lachowicz P., Zdziarski A. A., Schwarzenberg-Czerny A., Pooley G. G., Kitamoto S., 2006, MNRAS, 368, 1025
- Lamb R. C., Godfrey C. P., Wheaton W. A., Tumer T., 1982, Nat, 296, 543
- Malzac J., Belmont R., 2008, MNRAS, submitted
- Malzac J., Lubiński P., Zdziarski A. A., Cadolle Bel M., Türler M., Laurent P., 2008, A&A, in press (M08)
- Maraschi L., Treves A., 1981, MNRAS, 194, 1
- Protheroe, R. J. 2004, Astroparticle Phys., 21, 415
- Sikora, M., Begelman, M. C., & Rees, M. J. 1994, ApJ, 421, 153
- Stirling A. M., Spencer R. E., de la Force C. J., Garrett M. A., Fender R. R., Ogley R. N., 2001, MNRAS, 327, 1273
- Türler M. et al., 2006, ATel, 911, 1
- Wade G. A., Fullerton A. W., Donati J.-F., Landstreet J. D., Petit P., Strasser S., 2006, A&A, 451, 195
- Weekes T. C., 1983, A&A, 121, 232
- Zdziarski A. A., 1988, ApJ, 335, 786
- Zdziarski A. A., Poutanen J., Paciesas W. S., Wen L., 2002, ApJ, 578, 357
- Zdziarski A. A., Neronov A., Chernyakova M., 2008, arXiv:0802.1174
- Ziółkowski J., 2005, MNRAS, 358, 851